

## Lateral-torsional buckling steel beams with simultaneously tapered flanges and web

Juliusz Kuś\*

Faculty of Civil Engineering, Opole University of Technology, 45-758 Opole, Prószkowska Street 76, Poland

(Received September 04, 2014, Revised January 28, 2015, Accepted March 06, 2015)

**Abstract.** A procedure for critical buckling moment of a tapered beam is proposed with the application of potential energy calculations using Ritz method. Respective solution allows to obtain critical moments initiating lateral buckling of the simply supported, modestly tapered steel I-beams. In particular, lateral-torsional buckling of beams with simultaneously tapered flanges and the web are considered. Detailed, numerical, parametric analyses are carried out. Typical engineering, uniformly distributed design loads are considered for three cases of the load, applied to the top flange, shear centre, as well as to the bottom flange. In addition simply supported beam under gradient moments is investigated. The parametric analysis of simultaneously tapered beam flanges and the web, demonstrates that tapering of flanges influences much more the critical moments than tapering of the web.

**Keywords:** tapered I-beam; stability; lateral-torsional buckling; critical buckling moments

---

### 1. Introduction

Steel beams or columns tapered along their length or height are commonly applied in civil engineering because of their more optimal capabilities to carry on typical loads. This is particularly true when they are applied for middle size structures like industrial halls, trade malls, small bridges etc. That is why these type of steel structures are subjected of intensive research recently (see e.g., Marques *et al.* 2013, Benyamina *et al.* 2013, Yuan *et al.* 2013, Asgarian *et al.* 2013).

When properly designed against lateral torsional buckling, the steel beams are very economical in practical applications. However if these beams are not sufficiently resistant against flexural-torsional or lateral buckling their load capacity may substantially be reduced.

Stability of steel beams with linearly varying cross-sections along their length was analyzed by a relatively narrow group of specialists, though initial research on this problem started as early as in the fifties and sixties of the twentieth century. Butler (1966) presented the results of experimental I-section steel beams and channel sections with variable cross-section. Kitipornchai and Trahair (1972) gave approximate formulas for calculating the critical load initiating loss of stability of steel beams with tapered cross sections. The authors on the latter study also conducted an experiment on simply supported aluminium tapered I-beams. They found good agreement between their experimental results and the results of critical loads obtained from the analytical

---

\*Corresponding author, Ph.D., E-mail: [j.kus@po.opole.pl](mailto:j.kus@po.opole.pl)

formulas.

Finite Difference Method was applied to the solution of the problem of stability of tapered steel beams by Brown (1981). Wang *et al.* (1986), and Saka (1997) presented in their work the problem of optimal shape of tapered webs of steel beam with respect to the maximum critical load.

Probably the first attempt of applying the Finite Element Method (FEM) in determining the critical load of tapered steel beams was presented by Yang and Yau (1997). In their FEM model they took into account an uneven bending, using shell theory. These authors propose a formula with succeeding terms of stiffness matrix, which may be possible to solve the respective stability problem. The obtained results were compared with existing experimental results of Kitipornchai and Trahair (1972). Further applications of FEM in solving the beam stability problems were presented by Bradford (1988), as well as Bradford and Cuk (1988). These researchers proposed matrices of rigidity and inertia of the beam finite elements which takes into account variations of the cross-section along the beam. Good agreement of their analytical solutions was confirmed with the experiments of Kitipornchai and Trahair (1972) for simply supported beam and a cantilever. A similar problem was also solved by Gupta *et al.* (1996). Another simplified method for determining the critical load to cover variations of the web of the beam was published by Raftoyiannis and Ermopoulos (2005). Comprehensive publication on the stability of steel beams with tapered webs was presented by Andrade *et al.* (2007). In their work they applied the Rayleigh - Ritz method to determine the critical load of simply supported beams and cantilevers, for two types of convergence of the web for various spans. A comparison of their results with FEM program ABAQUS showed a good agreement. The extension of the above studies was made by Zhang and Tong (2008). They proposed, an expression describing the potential energy in the beam with tapered web. Their formula for total potential energy include terms depending on the angle of inclination of the beam shelf to its axis. They also examined two cases of converging beams using ANSYS FEM software, comparing respective results of calculations.

Recently Asgarian *et al.* (2013) and Benyamina *et al.* (2013) published papers on the stability of tapered beams limiting their research to the problem of tapered web. The paper by Asgarian *et al.* (2013) is devoted to the issue of stability of beams with arbitrary open cross-sections. These authors applied the method of power series to determine the critical lateral-torsional buckling of simply supported beams and cantilevers. It was demonstrated that when the number of power series terms exceeded 12, the difference between consecutive solutions was less than 1%. However they did not reveal exactly how the geometric section features along the beam length are changing. They analyzed the same load cases and patterns of convergence as in the paper by Andrade *et al.* (2007), showing good agreement of the results with existing solutions. The second recent paper on the stability of tapered beams was written by Benyamina *et al.* (2013) and was limited to beams with tapered web. They proposed a non-linear formula based on 1D model, which takes into account new kinematic relationships. Web tapered I-beam under uniformly distributed load was investigated for one scheme of convergence. This load was applied to the upper and lower flanges, as well as to the shear center. Also simply supported beam with tapered cross-section, under gradient moments at both ends was analyzed. The results were compared with the available previous literature output, demonstrating good agreement.

The purpose of this paper is to apply the Ritz method to obtain the critical lateral-torsional buckling moments for modestly tapered beams. Unlike in the previous papers, this time simultaneous changes of the web height and flange width are considered. This was obtained by defining two separate parameters describing web variations ( $\alpha_{TP}$ ) and changes in the flanges

width ( $\beta_{TP}$ ). Respective formula for the critical buckling moment depending on these parameters is derived and applied in detailed parametric study.

## 2. A model of bisymmetric tapered I-beam

### 2.1 Geometrical properties of tapered cross-section

Geometrical properties of beams with tapered cross-sections depend on parameters which define their shape. In this paper following two parameters were chosen:  $\alpha_{TP}$  to describe the web and  $\beta_{TP}$  for flanges. This parameters can be change simultaneously in all the calculations. These parameters are described in detail in Fig. 1 together with the initial cross-sectional characteristics defined as follows

$$A_0 = (2b_{f0}t_f + h_{w0}t_w) \tag{1}$$

$$I_{T0} = \frac{1}{3}(2b_{f0}t_f^3 + h_{w0}t_w^3) \tag{2}$$

$$I_{z0} = \frac{1}{6}b_{f0}^3t_f \tag{3}$$

$$I_{\omega0} = I_{z0} \frac{h_{d0}^2}{4} \tag{4}$$

It is assumed that the tapering of the beams analyzed in this paper is limited only to twice the cross-section size at both support. When parameters  $\alpha_{TP}$  and  $\beta_{TP}$  equals zero, the beam is prismatic

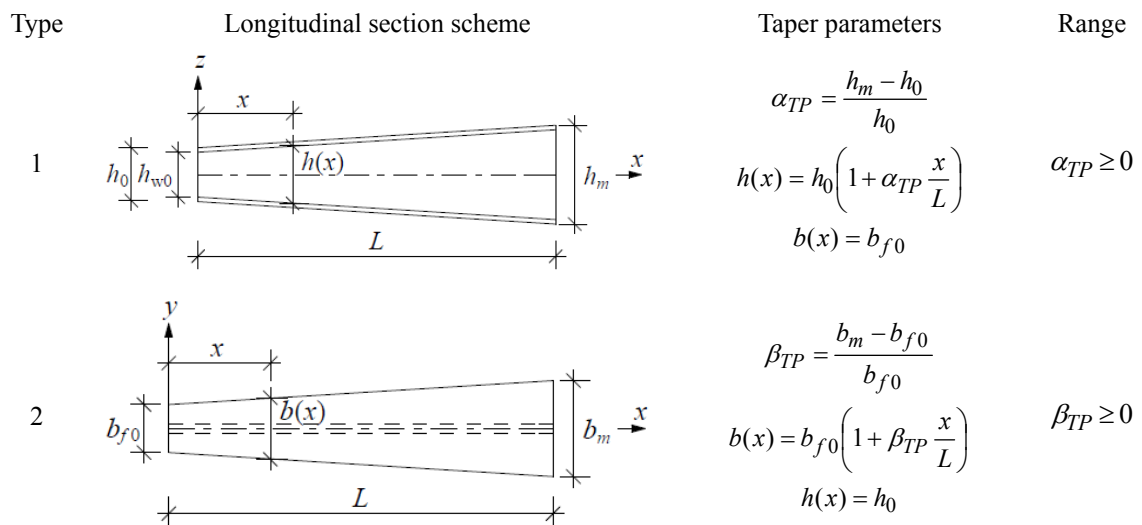


Fig. 1 Geometrical properties of beam with tapered web and flanges

with constant values of dimensions  $h_0$  and  $b_{f0}$  along the beam (uniform shape). The maximum tapering takes place when the support cross-section is twice as big as the left support. In this case it is assumed that the taper parameter takes value equal to 1.

Assuming that the thickness of the web and flanges are constant along the length of the beam, the characteristics of any geometrical cross-section varying over the length, can be expressed as follows

$$A(x) = A_0 + (2b_{f0}t_f\beta_{TP} + h_{w0}t_w\alpha_{TP})\left(\frac{x}{L}\right) \quad (5)$$

$$I_T(x) = I_{T0} + \frac{1}{3}(2b_{f0}t_f^3\beta_{TP} + h_{w0}t_w^3\alpha_{TP})\left(\frac{x}{L}\right) \quad (6)$$

$$I_y(x) = I_{y0} \left( 1 + (\beta_{TP} + 5\alpha_{TP})\left(\frac{x}{L}\right) + (4\alpha_{TP}^2 + 2\alpha_{TP}\beta_{TP})\left(\frac{x}{L}\right)^2 + (\alpha_{TP}^3 + \alpha_{TP}^2\beta_{TP})\left(\frac{x}{L}\right)^3 \right) \quad (7)$$

$$I_z(x) = I_{z0} \left( 1 + 3\beta_{TP}\left(\frac{x}{L}\right) + 3\beta_{TP}^2\left(\frac{x}{L}\right)^2 + \beta_{TP}^3\left(\frac{x}{L}\right)^3 \right) \quad (8)$$

$$I_\omega(x) = I_{\omega0} \left( 1 + (\beta_{TP} + 2\alpha_{TP})\left(\frac{x}{L}\right) + (\alpha_{TP}^2 + 3\beta_{TP}^2 + 6\alpha_{TP}\beta_{TP})\left(\frac{x}{L}\right)^2 + (3\alpha_{TP}^2\beta_{TP} + 6\beta_{TP}^2\alpha_{TP} + \beta_{TP}^3)\left(\frac{x}{L}\right)^3 + (3\beta_{TP}^2\alpha_{TP}^2 + 2\beta_{TP}^3\alpha_{TP})\left(\frac{x}{L}\right)^4 + \beta_{TP}^3\alpha_{TP}^2\left(\frac{x}{L}\right)^5 \right) \quad (9)$$

In these equations  $A(x)$  is the cross section area,  $I_T(x)$  is the torsion constant of the cross-section,  $I_y(x)$ ,  $I_z(x)$  are principal moment of inertia about  $y$  and  $z$  axes,  $I_\omega(x)$  is the warping constant,  $h_{w0}$  is the height of web,  $t_w$  is the web thickness,  $t_f$  is the flange thickness.

## 2.2 Total potential energy for beam with tapered cross-section

In this paper the functional for the total potential energy of the beam, commonly available in the literature (Benyamina *et al.* 2013, Andrade *et al.* 2007, Bradford and Cuk 1988) was used. In addition, components for total potential energy depending on the strain energy in web and flanges, due to their rotation and displacement during lateral buckling, were included (Bradford and Cuk 1988). Similar derivations of the components of the potential energy functional can be found in the papers by Benyamina *et al.* 2013 and Andrade *et al.* (2007).

Key element of present paper is now an introduction of the parameters defining the tapering of

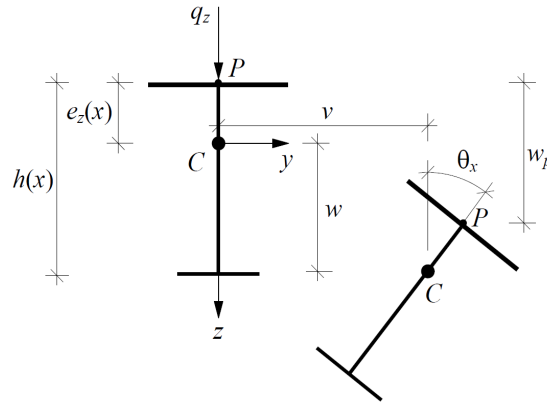


Fig. 2 I-section under lateral-torsional buckling

the web  $\alpha_{TP}$  and flanges  $\beta_{TP}$  into the integrands of the potential energy.

In Fig. 2,  $u$ ,  $v$ ,  $w$  are the displacement components of the shear centre point in the  $x$ ,  $y$  and  $z$  directions,  $\theta_x$  is the twist angle.

$$\begin{aligned}
 \Pi_{LTB} = & \frac{1}{2} \int_L \left( EI_z(x) \left( \frac{\partial^2 v}{\partial x^2} \right)^2 + GI_T(x) \left( \frac{\partial \theta_x}{\partial x} \right)^2 + EI_\omega(x) \left( \frac{\partial^2 \theta_x}{\partial x^2} \right)^2 \right) dx \\
 & + \frac{1}{2} \int_L \left( EI_z(x) \left( \left( \frac{\partial h(x)}{\partial x} \right)^2 \left( \frac{\partial \theta_x}{\partial x} \right)^2 + h(x) \left( \frac{\partial h(x)}{\partial x} \right) \left( \frac{\partial \theta_x}{\partial x} \right) \left( \frac{\partial^2 \theta_x}{\partial x^2} \right) \right) dx \\
 & + \int_L \left( (EI_{zt}(x) - EI_{zb}(x)) \left( \frac{\partial h(x)}{\partial x} \right) \left( \frac{\partial^2 v}{\partial x^2} \right) \left( \frac{\partial \theta_x}{\partial x} \right) \right) dx \\
 & + \int_L M_y \left( \theta_x \left( \frac{\partial^2 v}{\partial x^2} \right) \right) dx + \frac{1}{2} \int_L q_z e_z(x) \theta_x^2 dx
 \end{aligned} \tag{10}$$

Where  $I_{zt}(x)$  is moment of inertia of the tension flange,  $I_{zb}(x)$  is moment of inertia of the compression flange

### 3. General solution for critical buckling moments using Ritz method

Introducing discretization into the integral formulas (10), the problem is brought to systems of algebraic equations with unknowns parameters  $a_i$ , assumed for basis shape functions  $\theta_i$ .

$$\xi_n = \sum_{i=1}^n a_i \theta_i \tag{11}$$

When it comes to the state of static equilibrium of the beam, the potential energy takes a minimum value, so the parameters  $a_i$  can be determined with following extreme conditions

$$\frac{\partial \Pi_{LTB}(\xi_n)}{\partial a_i} = 0 \quad \text{for } i = 1, 2, \dots, n \quad (12)$$

To solve the stability problems using variational calculus method, proper functions  $\theta_i$  should be adopted to reflect the appropriate shape of the element axis after lateral buckling. These functions are limited in this paper to the shape characterising for simply supported I-beams. For this model the boundary conditions are defined as follows

$$\begin{aligned} v(0) = v(L) = 0, \quad \theta_x(0) = \theta_x(L) = 0 \\ v''(0) = v''(L) = 0, \quad \theta_x''(0) = \theta_x''(L) = 0 \end{aligned} \quad (13)$$

Now the Ritz functions can be defined. For this purpose trigonometric functions satisfying the boundary conditions (13) are defined as follows

$$v = \sum_{i=1}^n v_i \sin\left(i\pi \frac{x}{L}\right) \quad (14)$$

$$\theta_x = \sum_{i=1}^n \theta_i \sin\left(i\pi \frac{x}{L}\right) \quad (15)$$

Application of a finite number of elements of the sum in the expressions (14-15) leads to formal substitution of a continuous model by the discrete one. In order to obtain the desired level of accuracy of the calculations one must take a sufficiently large number of the elements. For practical, engineering, design calculations of simply supported beams, the critical buckling load can sufficiently be estimated using the first approximation ( $i = 1$ ).

In order to determine the critical buckling load, function of the gradient of the bending moment, depending on the load of the beam

$$m(x) = \frac{M_y}{M} \quad (16)$$

should be introduced into the potential energy functional (10). In equation (16) symbol  $M_y$  stands for the actual bending moment while  $M$  represents maximum bending moment in static equilibrium, during the state of the loss of stability critical buckling moment.

Finally following form for the potential energy with Ritz functions (14-15) is derived

$$\begin{aligned} \Pi_{LTB} = & \frac{1}{2} \int_0^L \left( EI_z(x) \left( \frac{\partial^2}{\partial x^2} \left( \sum_{i=1}^n v_i \sin\left(\frac{i\pi x}{L}\right) \right) \right)^2 + GI_T(x) \left( \frac{\partial}{\partial x} \left( \sum_{i=1}^n \theta_i \sin\left(\frac{i\pi x}{L}\right) \right) \right)^2 \right) dx \\ & + \frac{1}{2} \int_0^L \left( EI_\omega(x) \left( \frac{\partial^2}{\partial x^2} \left( \sum_{i=1}^n \theta_i \sin\left(\frac{i\pi x}{L}\right) \right) \right)^2 \right) dx \\ & + \frac{1}{2} \int_0^L \left( EI_z(x) \left( \left( \frac{\partial h(x)}{\partial x} \right)^2 \left( \frac{\partial}{\partial x} \left( \sum_{i=1}^n \theta_i \sin\left(\frac{i\pi x}{L}\right) \right) \right)^2 \right) \right) dx \end{aligned} \quad (17)$$

$$\begin{aligned}
 & + \frac{1}{2} \int_0^L \left( h(x) \left( \frac{\partial h(x)}{\partial x} \right) \left( \frac{\partial}{\partial x} \left( \sum_{i=1}^n \theta_i \sin \left( \frac{i\pi x}{L} \right) \right) \right) \left( \frac{\partial^2}{\partial x^2} \left( \sum_{i=1}^n \theta_i \sin \left( \frac{i\pi x}{L} \right) \right) \right) \right) dx \\
 & + \int_0^L \left( (EI_{zt}(x) - EI_{zb}(x)) \left( \frac{\partial h(x)}{\partial x} \right) \left( \frac{\partial^2}{\partial x^2} \left( \sum_{i=1}^n v_i \sin \left( \frac{i\pi x}{L} \right) \right) \right) \left( \frac{\partial}{\partial x} \left( \sum_{i=1}^n \theta_i \sin \left( \frac{i\pi x}{L} \right) \right) \right) \right) dx \\
 & + \overline{M} \int_0^L \left( m(x) \left( \sum_{i=1}^n \theta_i \sin \left( \frac{i\pi x}{L} \right) \right) \left( \frac{\partial^2}{\partial x^2} \left( \sum_{i=1}^n v_i \sin \left( \frac{i\pi x}{L} \right) \right) \right) \right) dx \\
 & + \frac{1}{2} \int_0^L \left( q_z e_z(x) \left( \sum_{i=1}^n \theta_i \sin \left( \frac{i\pi x}{L} \right) \right)^2 \right) dx
 \end{aligned} \tag{17}$$

Expression (17) can be written in a more concise form as follows

$$\Pi_{LTB} = \sum_{i=1}^n \left( k_{bb(m \times m)} v_i^2 + k_{cc(n \times n)} \theta_i^2 + k_{bc(m \times n)} v_i \theta_i \right) \tag{18}$$

Applying, in accordance with the Ritz method, minimization of the functional of total potential energy (17) using conditions

$$\frac{\partial \Pi_{LTB}}{\partial v_i} = 0, \quad i = 1, 2, 3, \dots, m \tag{19a}$$

$$\frac{\partial \Pi_{LTB}}{\partial \theta_i} = 0, \quad i = 1, 2, 3, \dots, n \tag{19b}$$

the following system of homogeneous, algebraic equations is obtained

$$\left[ \begin{array}{c|c} k_{bb(m \times m)} & k_{bc(m \times n)} \\ \hline sym & k_{cc(n \times n)} \end{array} \right] \begin{Bmatrix} v_{i(m \times 1)} \\ \theta_{i(n \times 1)} \end{Bmatrix} = \begin{Bmatrix} 0 \\ 0 \end{Bmatrix} \tag{20}$$

The components of the determinant of the matrix Eq. (20) for the first iteration ( $i = m = n = 1$ ) take form

$$k_{bb} = \frac{1}{2} \left( \frac{\pi}{L} \right)^4 E \int_0^L \left( I_z(x) \sin^2 \left( \frac{\pi x}{L} \right) \right) dx \tag{21}$$

$$\begin{aligned}
 k_{cc} = & \frac{1}{2} \left( \frac{\pi}{L} \right)^2 G \int_0^L \left( I_T(x) \cos^2 \left( \frac{\pi x}{L} \right) \right) dx + \frac{1}{2} \left( \frac{\pi}{L} \right)^4 E \int_0^L \left( I_\omega(x) \sin^2 \left( \frac{\pi x}{L} \right) \right) dx \\
 & + \frac{1}{2} \left( \frac{\pi}{L} \right)^2 E \int_0^L \left( I_z(x) \left( \left( \frac{\partial h(x)}{\partial x} \right)^2 \left( \cos^2 \left( \frac{\pi x}{L} \right) \right) \right) \right) dx
 \end{aligned} \tag{22}$$

$$\begin{aligned}
& + \frac{1}{2} \left( \frac{\pi}{L} \right)^3 E \int_0^L \left( I_z(x) h(x) \left( \frac{\partial h(x)}{\partial x} \right) \left( \cos \left( \frac{\pi x}{L} \right) \right) \left( \sin \left( \frac{\pi x}{L} \right) \right) \right) dx \\
& + \overline{M} \left( \frac{\pi}{L} \right)^2 \int_0^L \left( m(x) \beta_z(x) \cos^2 \left( \frac{\pi x}{L} \right) \right) dx + \frac{1}{2} q_z \int_0^L \left( e_z(x) \sin^2 \left( \frac{\pi x}{L} \right) \right) dx
\end{aligned} \tag{22}$$

$$\begin{aligned}
k_{bc} & = \left( \frac{\pi}{L} \right)^2 E \int_0^L \left( (I_{za}(x) - I_{zb}(x)) \left( \frac{\partial h(x)}{\partial x} \right) \left( \cos \left( \frac{\pi x}{L} \right) \right) \left( \sin \left( \frac{\pi x}{L} \right) \right) \right) dx \\
& + \overline{M} \left( \frac{\pi}{L} \right)^2 \int_0^L \left( m(x) \sin^2 \left( \frac{\pi x}{L} \right) \right) dx
\end{aligned} \tag{23}$$

The determinant of formula (20) equals the smallest, zero value for the critical moment  $M_{cr}$  which initiates loss of stability of the beam. The solution of Eq. (20) takes form of the familiar square polynomial with the unknowns  $\pm M$ . Detailed definition of critical moment  $M_{cr}$  depends on the external loads and geometrical features of the beam. Detailed examples are given in Section 5 of this paper.

#### 4. Application for tapered beam under different load cases

##### 4.1 I-beam with tapered cross-section with uniformly distributed load

Simply supported beam with uniformly distributed load was adopted as shown in Fig. 3. In this case formula (16) takes following form

$$m(x) = 4 \left( \frac{x}{L} - \frac{x^2}{L^2} \right) \tag{24}$$

while the maximum bending moment in the beam equals

$$M_{\max} = \frac{q_z L^2}{8} \tag{25}$$

and actual bending moment in the beam equals

$$M_y(x) = \frac{q_z L^2}{2} \left( \frac{x}{L} - \frac{x^2}{L^2} \right) \text{ for } 0 \leq x \leq L \tag{26}$$

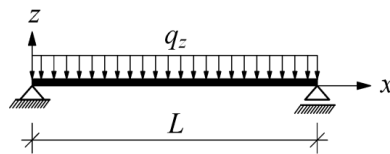


Fig. 3 Scheme beam with uniformly distributed load

The components of the matrix (20), taking into account formula (24) and the characteristics of the beam shown in Fig. 1 are

$$k_{bb} = \frac{1}{2} \int_0^L \left( EI_z(x) \frac{\pi^4 \sin^2\left(\frac{\pi x}{L}\right)}{L^4} \right) dx \tag{27}$$

$$k_{cc} = \frac{1}{2} \int_0^L \left( GI_T(x) \frac{\pi^2 \cos^2\left(\frac{\pi x}{L}\right)}{L^2} + EI_\omega(x) \frac{\pi^4 \sin^2\left(\frac{\pi x}{L}\right)}{L^4} \right) dx + \frac{1}{2} \int_0^L \left( EI_z(x) \left( \left( \frac{\partial h(x)}{\partial x} \right)^2 \frac{\pi^2 \cos^2\left(\frac{\pi x}{L}\right)}{L^2} + h(x) \frac{\partial h(x)}{\partial x} \frac{\pi^3 \sin^2\left(\frac{2\pi x}{L}\right)}{L^3} \right) \right) dx \tag{28}$$

$$+ 4\bar{M} \int_0^L \left( \left( \frac{x}{L} - \frac{x^2}{L^2} \right) \beta_z(x) \frac{\pi^2 \cos^2\left(\frac{\pi x}{L}\right)}{L^2} \right) dx + \frac{1}{2} \int_0^L \left( q_z e_z(x) \sin^2\left(\frac{\pi x}{L}\right) \right) dx$$

$$k_{bc} = \int_0^L \left( E(I_{zt}(x) - I_{zb}(x)) \left( \frac{\partial h(x)}{\partial x} \frac{\pi^3 \sin^2\left(\frac{2\pi x}{L}\right)}{2L^3} \right) \right) dx + \bar{M} \int_0^L \left( \left( \frac{x}{L} - \frac{x^2}{L^2} \right) \frac{\pi^2 \sin^2\left(\frac{\pi x}{L}\right)}{L^2} \right) dx \tag{29}$$

Setting the integrand expressions, taking into account the geometric parameters of the tapered beam for various patterns of tapering (Fig. 1), matrix elements (20) were obtained. Finally the particular solution Eq. (20) for the simply supported beam under uniformly distributed load equals

$$\det \begin{bmatrix} k_{bb} & k_{bc} \\ sym & k_{cc} \end{bmatrix} = 0 \tag{30}$$

Solution of Eq. (30) with respect to moment  $M$ , leads to the determination of the critical buckling moments initiating loss of stability. This solution will be used in calculation examples of Section 5.

#### 4.2 I-beam with tapered cross-section under positive gradient moments

Simply supported beam under positive gradient moments was considered as shown in Fig. 4. In this case formula (16) takes following form

$$M_y(x) = M \left( \psi - \frac{1}{L}(\psi - 1)x \right) \quad \text{for } 0 \leq \psi < 1 \tag{31}$$

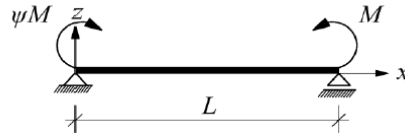


Fig. 4 Scheme beam under positive gradient moments

while the maximum bending moment in the beam equals

$$M_{\max} = M \tag{32}$$

and actual bending moment in the beam equals

$$m(x) = \psi - \frac{1}{L}(\psi - 1)x \quad \text{for } 0 \leq \psi < 1 \tag{33}$$

The components of the matrix (20), taking into account formula (31) and the characteristics of the beam shown in Fig. 1 are

$$k_{bb} = \frac{1}{2} \int_0^L \left( EI_z(x) \frac{\pi^4 \sin^2\left(\frac{\pi x}{L}\right)}{L^4} \right) dx \tag{34}$$

$$k_{cc} = \frac{1}{2} \int_0^L \left( GI_T(x) \frac{\pi^2 \cos^2\left(\frac{\pi x}{L}\right)}{L^2} + EI_\omega(x) \frac{\pi^4 \sin^2\left(\frac{\pi x}{L}\right)}{L^4} \right) dx + \frac{1}{2} \int_0^L \left( EI_z(x) \left( \left( \frac{\partial h(x)}{\partial x} \right)^2 \frac{\pi^2 \cos^2\left(\frac{\pi x}{L}\right)}{L^2} + h(x) \frac{\partial h(x)}{\partial x} \frac{\pi^3 \sin^2\left(\frac{2\pi x}{L}\right)}{L^3} \right) \right) dx \tag{35}$$

$$+ \overline{M} \int_0^L \left( \left( \psi - \frac{1}{L}(\psi - 1)x \right) \beta_z(x) \frac{\pi^2 \cos^2\left(\frac{\pi x}{L}\right)}{L^2} \right) dx$$

$$k_{bc} = \overline{M} \int_0^L \left( \left( \psi - \frac{1}{L}(\psi - 1)x \right) \frac{\pi^2 \sin^2\left(\frac{\pi x}{L}\right)}{L^2} \right) dx. \tag{36}$$

Using the same procedure as mentioned in paragraph 4.1 matrix elements (20) were calculated and in next step critical buckling moments for beam under positive moment gradient were

computed. Detailed examples are shown in section 5 of this paper.

## 5. Applications and results of calculations

The purpose of this chapter is to check the accuracy of solutions obtained by the method proposed in Chapter 4, in comparison with the finite element approach as well as to carry on a parametric analysis. Steel beams are assumed to be made of steel with Young's modulus of  $E = 210$  GPa, modulus of Kirchoff  $G = 81$  GPa, i.e., Poisson's ratio = 0.3.

The verifying computations were performed using the ANSYS FEM software system. A rod "BEAM188" finite element was assumed. It is a two-node element with seven degrees of freedom - three translational UX, UY, UZ, three rotary ROTX, ROTY, ROTZ and seventh optional degree of freedom to restrict the freedom of cross-sectional warping. The beam supports were modeled by blocking translational degrees of freedom UY = 0, UZ = 0 and locking the axial rotation degree of freedom ROTX = 0.

### 5.1 Example 1 – I-beam with tapered flanges

In this example, critical buckling moments of simply supported steel bisymmetrical I-beam with tapered flanges and uniform web was investigated. The beam span varied from 6 to 12 m, the taper parameter changed from  $\beta_{TP} = 0$  (prismatic beam) to  $\beta_{TP} = 1$  ( $b_m = 2b_{f0}$ ), the load was applied to the shear center, the upper flange and the lower flange. The difference between the values of the critical buckling moments, calculated using the Ritz method, and those of the ANSYS program were determined according to the formula.

$$\Delta = \left| \frac{M_{cr}^{Ritz} - M_{cr}^{Ansys}}{M_{cr}^{Ansys}} \right| \cdot 100\% \quad (37)$$

Tables 2A-2C summarize the critical buckling moments for beams with taper flanges for the tapering parameter  $\beta_{TP} = 0 \div 1$ , as well as for different variants of the application of the load on the section height.

First the results using formula (30) and the FEM solutions are compared. In all the three analyzed cases (beams with spans 6, 9 and 12 m), the critical buckling moments calculated using the formula (30) revealed sufficient accuracy (Tables 2A-2C).

For beam with a load on the upper flange ( $e_z(x) = 0.15$  m), the maximum difference between the critical moments calculated by Ritz method, and in the program ANSYS were up 7%, respectively, for the scheme of Fig. 3(b) ( $e_z(x) = 0, 0$  m) - 3.8%, and Fig. 3(c) ( $e_z(x) = -0.15$  m) - 10.7%.

Next a parametric analysis with respect to flange tapering  $\beta_{TP}$  is carried out. It can be seen that the convergence of the flanges has a significant influence on the growth of critical buckling moments (Tables 2A-2C) with respect to the prismatic beam (Tables 2A-2C,  $\beta_{TP} = 0.0$ ). For the load applied to the upper flange and the tapering parameter  $\beta_{TP} = 0.4$  the increase of critical buckling moment equals approx. 32%, while for the tapering parameter  $\beta_{TP} = 1.0$  up to 64%, relative to prismatic beam with  $\beta_{TP} = 0.0$ .

For the remaining two spans of beam (9 m and 12 m), with the same parameters of flanges tapering the differences were similar.

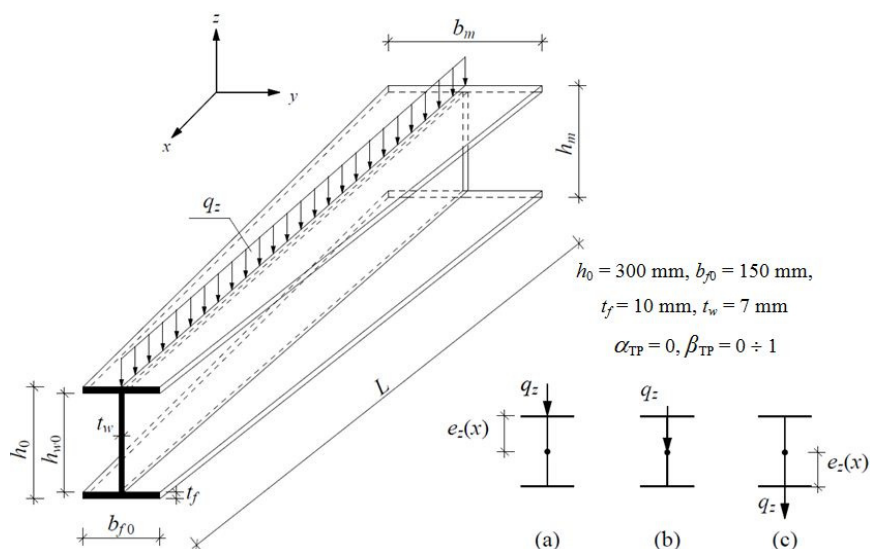


Fig. 4 Sketch showing a simply supported beam with tapered flanges, under distributed load applied to top flange (a), shear centre (b) and bottom flange (c)

Table 1A Critical buckling moments for simply supported beam with tapered flanges under distributed load (Fig. 4(a))

L (m)	$\beta_{TP}$	Load on top flange		
		Critical buckling moments (kNm)		$\Delta\%$
		Ritz method	Ansys	
6,0	0,0	64,08	64,39	0,5
	0,2	73,62	73,55	0,1
	0,4	84,64	87,62	3,4
	0,6	97,89	102,86	4,8
	0,8	113,83	119,31	4,6
	1,0	132,87	137,02	3,0
9,0	0,0	40,29	40,84	1,3
	0,2	46,45	46,87	0,9
	0,4	52,74	54,98	4,1
	0,6	59,86	63,48	5,7
	0,8	67,90	72,49	6,3
	1,0	77,35	82,12	5,8
12,0	0,0	30,24	30,51	0,9
	0,2	34,69	35,10	1,2
	0,4	39,23	40,86	4,0
	0,6	44,18	46,99	6,0
	0,8	49,63	53,35	7,0
	1,0	55,68	59,94	7,1

Table 1B Critical buckling moments for simply supported beam with tapered flanges under distributed load (Fig. 4(b))

$L$ (m)	$\beta_{TP}$	Load on shear centre		
		Critical buckling moments (kNm)		$\Delta\%$
		Ritz method	Ansys	
6,0	0,0	86,45	86,70	0,3
	0,2	102,81	103,09	0,3
	0,4	122,12	124,96	2,3
	0,6	145,24	148,86	2,4
	0,8	172,82	174,87	1,2
	1,0	205,45	203,17	1,1
9,0	0,0	51,22	51,17	0,1
	0,2	60,02	60,55	0,9
	0,4	70,19	72,29	2,9
	0,6	81,92	84,85	3,5
	0,8	95,46	98,31	2,9
	1,0	111,06	112,80	1,5
12,0	0,0	35,97	36,48	1,4
	0,2	42,55	43,02	1,1
	0,4	49,36	50,94	3,1
	0,6	57,01	59,22	3,7
	0,8	65,62	68,22	3,8
	1,0	75,32	77,74	3,1

Table 1C Critical buckling moments for simply supported beam with tapered flanges under distributed load (Fig. 4(c))

$L$ (m)	$\beta_{TP}$	Load on bottom flange		
		Critical buckling moments (kNm)		$\Delta\%$
		Ritz method	Ansys	
6,0	0,0	115,29	116,45	0,9
	0,2	143,41	138,54	3,5
	0,4	175,95	170,52	3,2
	0,6	215,15	205,76	4,6
	0,8	261,90	244,38	7,2
	1,0	317,06	286,48	10,7
9,0	0,0	63,58	64,07	0,8
	0,2	77,47	75,84	2,1
	0,4	93,32	91,88	1,6
	0,6	111,97	109,36	2,4
	0,8	133,81	128,29	4,3
	1,0	159,21	147,75	7,8

Table 1C Continued

L (m)	$\beta_{TP}$	Load on bottom flange		
		Critical buckling moments (kNm)		$\Delta\%$
		Ritz method	Ansys	
12,0	0,0	43,07	43,58	1,1
	0,2	52,14	51,46	1,3
	0,4	62,05	61,74	0,5
	0,6	73,49	72,85	0,9
	0,8	86,65	84,74	2,3
	1,0	101,73	97,56	4,3

5.2 Example 2 – I-beam with simultaneously tapered flanges and web

In the following example, critical buckling moments for simply supported steel I-beam with a cross section which has both tapered flanges and the web are analyzed. Span of the beam is set to 6 m, 9 m and 12 m. The tapering parameter of web and flanges changes from  $\alpha_{TP} = \beta_{TP} = 0$  (prismatic beam) to  $\alpha_{ip} = \beta_{ip} = 1$  ( $h_m = 2h_0, b_m = 2b_{f0}$ ).

The values of the critical moments are gathered in Tables 3A-3C. The load was applied to the shear centre, as well as to the upper and lower flanges.

First the accuracy of the solutions using formula (30) and the FEM ANSYS model are compared. Again the results using the Ritz method are in sufficient agreement with the results of the FEM analysis. In most cases it is about 0,2%-5% which is enough in practical engineering,

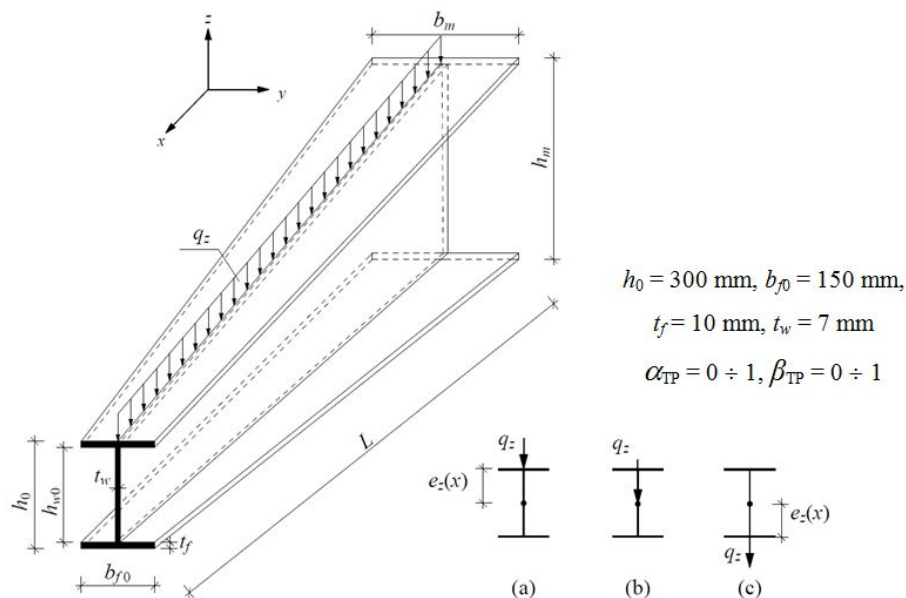


Fig. 5 Sketch showing a simply supported beam with simultaneously tapered web and flanges, under distributed load applied to top flange (a), shear centre (b) and the bottom flange (c)

Table 2A Critical buckling moments for simply supported beam with simultaneously tapered flanges and web under distributed load (Fig. 5(a))

$L$ (m)	$\alpha_{TP} = \beta_{TP}$	Load on top flange		
		Critical buckling moments (kNm)		$\Delta\%$
		Ritz method	Ansys	
6,0	0,0	64,4	64,3	0,1
	0,2	76,1	81,2	6,3
	0,5	102,9	111,4	7,6
	0,8	145,0	147,8	1,9
	1	184,1	175,8	4,7
	0,0	40,8	40,8	0
9,0	0,2	46,9	49,9	6,0
	0,5	59,6	65,2	8,7
	0,8	78,2	83,0	5,8
	1	95,2	96,3	1,2
	0,0	30,5	30,5	0
	0,2	34,7	36,8	5,6
12,0	0,5	42,7	47,0	9,1
	0,8	53,5	58,3	8,3
	1	63,1	66,7	5,3
	0,0	64,4	64,3	0,1
	0,2	76,1	81,2	6,3
	0,5	102,9	111,4	7,6

Table 2B Critical buckling moments for simply supported beam with simultaneously tapered flanges and web under distributed load (Fig. 5(b))

$L$ (m)	$\alpha_{TP} = \beta_{TP}$	Load on shear centre		
		Critical buckling moments (kNm)		$\Delta\%$
		Ritz method	Ansys	
6,0	0,0	86,7	85,9	0,9
	0,2	107,9	112,0	3,7
	0,5	154,4	161,0	4,1
	0,8	225,1	219,6	2,5
	1	289,5	266,3	8,7
	0,0	51,2	50,8	0,7
9,0	0,2	61,7	64,1	3,7
	0,5	83,4	87,7	4,8
	0,8	115,0	116,1	0,9
	1	143,3	138,0	3,9
	0,0	36,5	36,3	0,6
	0,2	43,3	45,0	3,7

Table 2B Continued

$L$ (m)	$\alpha_{TP} = \beta_{TP}$	Load on shear centre		
		Critical buckling moments (kNm)		$\Delta\%$
		Ritz method	Ansys	
12,0	0,5	56,5	59,9	5,7
	0,8	74,9	77,5	3,4
	1	90,9	90,8	0,2
	0,0	86,7	85,9	0,9
	0,2	107,9	112,0	3,7
	0,5	154,4	161,0	4,1

Table 2C Critical buckling moments for simply supported beam with simultaneously tapered flanges and web under distributed load (Fig. 5(c))

$L$ (m)	$\alpha_{TP} = \beta_{TP}$	Load on bottom flange		
		Critical buckling moments (kNm)		$\Delta\%$
		Ritz method	Ansys	
6,0	0,0	116,6	116,1	0,5
	0,2	152,4	154,2	1,2
	0,5	254,2	243,8	4,3
	0,8	348,4	325,6	7,0
	1	454,2	402,8	12,8
	0,0	64,1	63,8	0,4
9,0	0,2	83,1	82,3	1,0
	0,5	116,4	117,7	1,0
	0,8	168,6	162,0	4,0
	1	215,2	196,4	9,5
	0,0	43,6	43,4	0,4
	0,2	55,1	55,0	0,2
12,0	0,5	74,4	76,4	2,7
	0,8	104,3	102,8	1,5
	1	130,6	123,4	5,8
	0,0	116,6	116,1	0,5
	0,2	152,4	154,2	1,2
	0,5	254,2	243,8	4,3

design applications. The maximum difference did not exceed 10%.

As a result of this parametric analysis, it can be concluded that the simultaneous tapering of the flanges and web causes a significant increase of the critical lateral-torsional buckling moments.

Consider for example the results for the beam with the bottom flange loaded. For the tapering parameters  $\alpha_{TP} = \beta_{TP} < 0.5$  the increase of critical moments with respect to the prismatic beam assumption equals approx. 24%. For  $\alpha_{TP} = \beta_{TP} = 1.0$  the critical moment increases up to 75%.

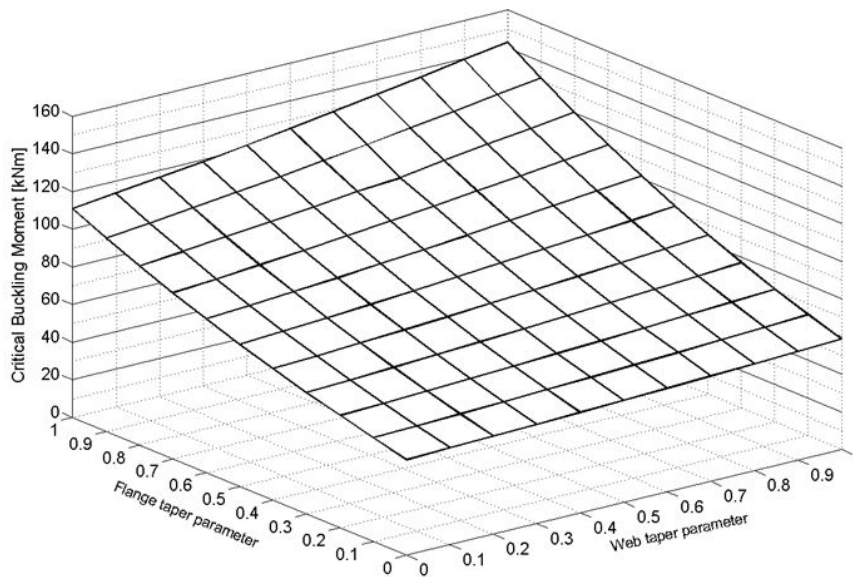


Fig. 6 Plot of critical buckling moments as a function of flange and web taper parameters (9 m span beam under uniformly distributed load applied to its shear centre)

In order to assess the influence of tapering of beam elements on critical buckling moments, a surface 3D plot has been prepared and presented in Fig. 6. The computations were carried out for a 9 m span beam under uniformly distributed load applied to the shear centre. In this plot the first, horizontal axis stands for the web taper parameter ( $\alpha_{TP}$ ), while the second one represents flange taper parameter ( $\beta_{TP}$ ).

The comparison between critical buckling moments calculated using formula (30) for different tapering parameters of beams elements, showed that the critical buckling moments are the most influenced in case of simultaneously tapered flanges and web. Tapering of web gives relatively small increase of the critical buckling moment. The difference between prismatic beam ( $\alpha_{TP} = 0$ ) and the web tapered beam ( $\alpha_{TP} = 1$ ) is about 11%. Similar differences of critical buckling moments for the web tapered beam can be found in the paper by Andrade *et al.* (2007). Beams with tapered flanges are more resistant to stability loss than beams with tapered web. For the same value of tapering parameter, difference between values of critical buckling moments for beam with tapered flanges ( $\beta_{TP} = 1$ ) and beam with tapered web ( $\alpha_{TP} = 1$ ) was about 59%.

### 5.3 Example 3 – I-beam with tapered cross-section under gradient moments

In the following example, critical buckling moments of two sets of simply supported beams with tapered cross-section, under gradient moments are addressed. In first case (Fig. 7(a)) flange-tapered cross-section is analyzed. Range of gradient moment varies from  $\Psi = 1$  to  $\Psi = 0,25$ . Flange width is changing from  $b_{f0} = 150$  mm to  $b_m = 300$  mm. Table 5 contains values of critical buckling moments compared with FE model in ANSYS.

Critical buckling moments evaluated by the presented method and FE model are in good agreement. Relative differences do not exceed more than 4%. As could be expected highest value of critical load have beams with taper parameter  $\beta_{TP}$  equal 1,0.

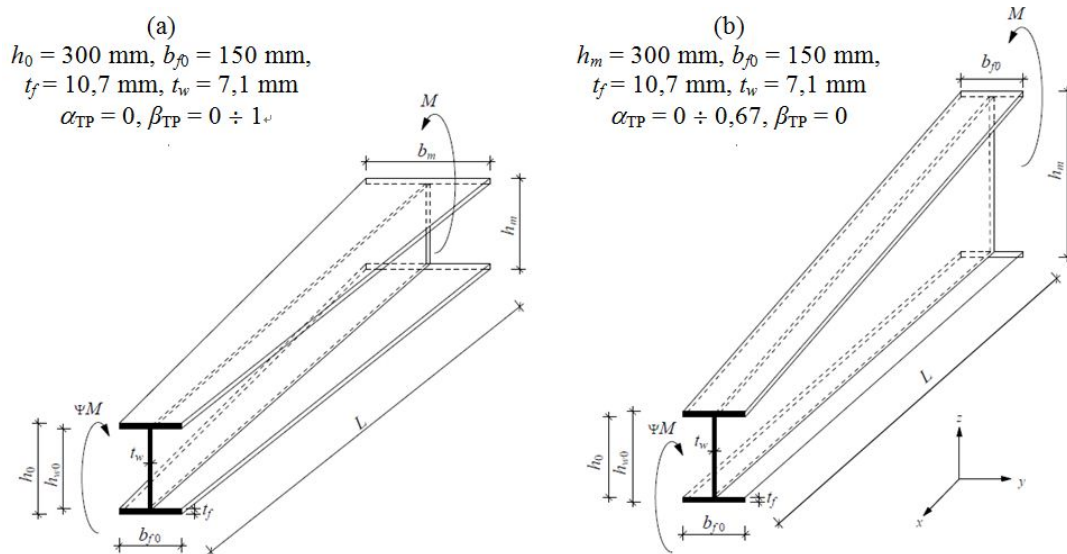


Fig. 7 Sketch showing a simply supported beam under gradient moments

Table 3 Critical buckling moments for simply supported flange-tapered beam under gradient moments (Fig. 7(a))

L (m)	$\beta_{TP}$	Critical buckling moment (kNm)							
		$\Psi = 0,25$		$\Psi = 0,5$		$\Psi = 0,75$		$\Psi = 1$	
		This paper	ANSYS	This paper	ANSYS	This paper	ANSYS	This paper	ANSYS
6,0	0,0	132,9	134,9	110,8	113,6	94,9	93,6	83,1	82,1
	0,25	164,2	166,7	136,9	140,3	117,3	119,8	102,6	104,3
	0,50	203,2	206,2	169,4	173,6	145,2	148,2	127	129,5
	0,75	251,7	251,3	209,8	203,8	179,8	185,9	157,3	158,6
	1,0	311,6	308,1	259,6	266,1	222,5	227,2	194,7	193,4
9,0	0,0	79,1	75,3	65,9	64,5	56,5	55,8	49,4	48,9
	0,25	96,4	100,2	80,3	84	68,8	71,6	60,2	62,1
	0,50	116,9	127,5	97,4	105,1	83,5	88,4	73	75,9
	0,75	141,2	141,7	117,7	115,1	100,8	95,8	88,2	81,7
	1,0	170,1	189	141,8	151,1	121,5	125,1	106,3	105,9

Second set (Fig. 7(b)) contains the beam with linear web tapering varying from  $h_0$  at left support to  $h_m$  at right support. In all six cases height of beam on left side was constant and takes value  $h_m = 300$  mm, height of the beam on left side was changing from  $h_0 = 180$  mm ( $\alpha_{TP} = 0,67$ ) to  $h_0 = 300$  mm ( $\alpha_{TP} = 0,0$ ) Gradient moment is varied from  $\Psi = 1$  (which correspond to uniform moment) to  $\Psi = 0,25$ . Two types of length are investigated. Table 6 gives results of calculations using proposed Ritz method with compare to existing values of critical buckling loads from paper by Benyamina *et al.* (2013).

Table 4 Critical buckling moments for simply supported web-tapered beam under gradient moments (Fig. 7(b))

L (m)	$\alpha_{TP}$	Critical buckling moment (kNm)							
		$\Psi = 0,25$		$\Psi = 0,5$		$\Psi = 0,75$		$\Psi = 1$	
		This paper	Benyamina <i>et al.</i> (2013)	This paper	Benyamina <i>et al.</i> (2013)	This paper	Benyamina <i>et al.</i> (2013)	This paper	Benyamina <i>et al.</i> (2013)
4,0	0,67	209,4	207,4	174,5	175,5	149,6	150,8	130,8	131,7
	0,25	224,9	220,1	186,9	186,9	160,2	161,1	140,2	140,9
	0,0	240,7	233,0	200,6	198,3	171,9	171,4	150,4	150,2
6,0	0,67	119,7	118,7	99,7	100,8	85,5	86,8	74,8	75,8
	0,25	125,9	123,5	105,0	105,0	90,0	90,7	78,8	79,3
	0,0	132,9	128,8	110,8	109,4	94,9	94,6	83,0	82,9

Comparing the results from the above table, it can be seen that proposed approximation is enough accurate for the tapered beam analyzed in the paper. Highest difference does not exceed more than 3%.

## 6. Conclusions

Results of the research on lateral torsional buckling problem of beams with simultaneously tapered flanges and webs are reported. A solution of this problem using the Ritz method is developed. It allows determining the critical lateral-torsional buckling moments for tapered beams.

Bisymmetrical I-beams with linearly changing flanges as well as with equally variable flanges widths and web heights were analysed, considering four load cases: with distributed load applied at the shear centre, at the upper flange and at the lower flange and under gradient moments.

It was observed that the values of critical buckling moment calculated using the applied implementation of the Ritz method (Eq. (30)) and the FEM approach, gave satisfactory agreement from an engineering point of view (mostly below 2% - only in three extreme cases reaching 10%).

As could be expected, the critical moments computed for the beams with converging flanges are significantly higher than the critical moments computed for prismatic beams (from 16% for  $\beta_{TP} = 0,2$  up to 64% for  $\beta_{TP} = 1,0$ ).

For beams with simultaneously tapered flanges widths and web height, the critical buckling moment increased by 70% ( $\alpha_{TP} = 1,0$ ,  $\beta_{TP} = 1,0$ ) compare to the beam with a prismatic cross-section for the same initial values of  $h_0$  and  $b_{f0}$  ( $\alpha_{TP} = \beta_{TP} = 0$ ). It may also be concluded that the simultaneous tapering of the flanges and the web generates a relatively small increase in the critical moments of the beams compare, to the tapered flanges. This increase equals respectively 30% and 17% for beams with a span of 6 m and 12 m.

Moreover, it can be seen that among the analyzed structural cases, tapering of web has the smallest influence for critical buckling moments of beams. Difference between values of critical buckling moments for prismatic beam and web tapered beam was about 11%.

It may be concluded that the application of the tapered flanges and web is particularly beneficial since these types of beams are not only lighter but also represent better load capacity with respect to the lateral torsional buckling.

## Acknowledgments

This paper contains main results of the Author's PhD thesis (Kus 2013). A partial support of the NBS 15/14 Grant of Polish Ministry of Science & Higher Education is gratefully acknowledged. The Author wishes to thank to prof. Jan Zmuda for inspiration and prof. Zbigniew Zembaty for detailed review of the manuscript in its early stage.

## References

- Andrade, A., Camotim, D., Borges Dinis, P. (2007), "Lateral-torsional buckling of singly symmetric web-tapered thin-walled I-beams: 1D model vs. Shell FEA", *Comput. Struct.*, **85**(17-18), 1343-1359.
- Asgarian, B., Soltani, M. and Mohri, F. (2013), "Lateral-torsional buckling of tapered thin-walled beams with arbitrary cross-sections", *Thin-Wall. Struct.*, **62**, 96-108.
- Benyamina, A.B., Meftah, S.A., Mohri, F. and Daya, E.M. (2013), "Analytical solutions attempt for lateral torsional buckling of double symmetric web-tapered I-beams", *Eng. Struct.*, **56**, 1207-1219.
- Bradford, M.A. (1988), "Stability of tapered I-beams", *J. Construct. Steel Res.*, **9**(3), 195-216.
- Bradford, M.A. and Cuk, P.E. (1988), "Elastic buckling of tapered monosymmetric I-beams", *J. Struct. Eng.*, **114**(5), 977-996.
- Brown, T.G. (1981), "Lateral torsional buckling of tapered I-beams", *J. Struct. Div., ASCE*, **107**, 689-697.
- Butler, D.J. (1966), "Elastic buckling on laterally and torsionally braced tapered beams", *Weld. J. Res. Suppl.*, **45**(1), 1-41.
- Gupta, P., Wang, S.T. and Blandford, G.E. (1996), "Lateral-torsional buckling of nonprismatic I-beams", *J. Struct. Eng.*, **122**(7), 748-755.
- Kitipornchai, S. and Trahair, N.S. (1972), "Elastic stability of tapered I-beams", *J. Struct. Div., ASCE*, **98**(3), 713-728.
- Kuś, J. (2013), "Stability of beams with tapered cross-sections", Ph.D. Dissertation; Faculty of Civil Engineering Opole University of Technology, pp. 1-92. [In Polish: Analiza stateczności belek ze zbieżnymi przekrojami poprzecznymi]
- Marques, L., da Silva, L.S., Greiner, R., Rebelo, C. and Taras, A. (2013), "Development of a consistent design procedure for lateral-torsional buckling of tapered beams", *J. Construct. Steel Res.*, **89**, 213-235.
- Raftoyiannis, I.G., Ermopoulos, J.Ch. (2005), "A stability of tapered and stepped steel columns with initial imperfections", *Eng. Struct.*, **27**(8), 1248-1257.
- Saka, M.P. (1997), "Optimum design of steel frames with tapered members", *Comput. Struct.*, **63**, 797-811.
- Wang, C.M., Thevendran, V., Teo, K.L. and Kitipornchai, S. (1986), "Optimal design of tapered beams for maximum buckling strength", *Eng. Struct.*, **8**(4), 276-284.
- Yang, W.B. and Yau, J.D. (1997), "Stability of beams with tapered I-sections", *J. Eng. Mech.*, **113**(9), 1337-1357.
- Yuan, W.B., Kim, B. and Chen, C.Y. (2013), "Lateral-torsional buckling of steel web tapered tee-section cantilevers", *J. Construct. Steel Res.*, **87**, 31-37.
- Zhang, L. and Tong, G.S. (2008), "Lateral buckling of web-tapered I-beams: A new theory", *J. Construct. Steel Res.*, **64**, 1379-1393.